A NEW IMAGE QUALITY METRIC USING COMPRESSIVE SENSING AND A FILTER SET CONSISTING OF DERIVATIVE AND GABOR FILTERS

Dong-O Kim and Rae-Hong Park

Department of Electronic Engineering, Sogang University, Seoul, Korea

ABSTRACT

This paper proposes an image quality metric (IQM) using compressive sensing (CS) and a filter set consisting of derivative and Gabor filters. In this paper, compressive sensing that is used for acquiring a sparse or compressible signal with a small number of measurements is used for measuring the quality between the reference and distorted images. However, an image is generally neither sparse nor compressible, so a CS technique cannot be directly used for image quality assessment. Thus, for converting an image into a sparse or compressible signal, the image is convolved with filters such as the gradient, Laplacian of Gaussian, and Gabor filters, since the filter outputs are generally compressible. A small number of measurements obtained by a CS technique are used for evaluating the image quality. Experimental results with various test images show the effectiveness of the proposed algorithm in terms of the Pearson correlation coefficient (CC), root mean squared error, Spearman rank order CC, and Kendall CC.

KEYWORDS

Compressive Sensing, Derivative Filters, Difference Mean Opinion Score, Gabor Filter, Image Quality Assessment

1. INTRODUCTION

Objective image quality assessment (IQA) has the goal to evaluate the quality of an arbitrary image, which coincides with the subjective image quality such as the mean opinion score (MOS). The MOS represents the image quality that follows the human visual perception. Since the subjective IQA has a drawback that a large number of images and evaluators are needed, the objective IQA is preferred and has been widely investigated [1–31]. The closer to the subjective IQA an objective IQA is, the better the image quality metric is. In general, objective IQA algorithms are classified into three approaches according to the type of information used: structure, human perception/visual attention, and information theory.

In most IQA methods, image representation techniques, based on image features, image histogram, and so on, have been widely used for assessing the image quality. However, in this paper, we adopt a new concept for assessing the image quality. That is, instead of an image representation technique, we use compressive sensing (CS) as a measurement technique that uses the implicit information of an image. In this paper, we present a new image quality metric (IQM) using CS and a filter set. The filter set consists of the gradient, Laplacian of Gaussian (LoG), and Gabor filters used for spectral analysis [32], in which an image is analyzed via several types of filters since each filter has a unique filter response. Also, derivative images or Gabor filtered

DOI : 10.5121/avc.2015.2101

images are generally sparse or compressible because the pixel values of those images are close to zero in relatively flat regions. A sparse or compressible signal can be implicitly represented as CS measurements.

The rest of this paper is organized as follows. Section 2 briefly introduces conventional IQA algorithms. Next, our proposed IQM using CS and a filter set consisting of derivative and Gabor filters is described in Section 3. Experimental results with LIVE database and TID2008 database are discussed in Section 4 and conclusions are given in Section 5.

2. RELATED WORK

Conventional IQMs can be classified into three categories: structural information based [2–17], human perception/visual attention based [18–28], and information theoretical approaches [29, 30]. In this section, conventional IQMs are reviewed.

2.1. Structural Information Based IQMs

Motivation of structural information based IQA is that the structural information of an image changes if an image is distorted. The universal quality index (UQI) [2] was presented as a full-reference (FR) IQM using the structural information of an image. The structural similarity (SSIM) [3], a modified version of the UQI, was also developed. However, the SSIM gives poor performance for badly blurred images. To reduce performance degradation, new methods were developed [4, 5]. Edge-based SSIM [4] is based on the edge information as the most important image structure information. The gradient-based SSIM has been proposed by noting the fact that the human visual system (HVS) is sensitive to changes of edges [5]. A multi-scale SSIM (MSSSIM) [6] was proposed as the extended version of the SSIM in terms of the scale. Also for video quality assessment, the SSIM was extended to the video SSIM (VSSIM) [7]. An IQA method based on the edge and contrast similarity between the reference and distorted images [8] was proposed by combining the edge similarity with the contrast similarity used in the SSIM. Similarly to the MSSSIM, an IQM based on multi-scale edge representation was proposed [9]. Also, a discrete wavelet transform-based SSIM [10] was proposed for IQA.

Shnayderman *et al.* proposed an image quality metric based on singular value decomposition (SVD) [11], which is called the MSVD. The MSVD method used the mean of the differences between SVD values for assessing the image quality. An IQM using LU factorization (MLU) was proposed, where LU factorization was used for representation of the structural information of an image [12]. An IQM based on Harris response (HRQM) was proposed, in which Harris response was computed from the gradient information matrix [13]. In [14], the joint feature similarity metric (JFSM) was presented, in which image pixels were classified into three structure types to effectively assess the visual quality. Also, feature map based IQM [15] was proposed based on the SSIM. Instead of comparing images directly, the method uses the SSIM in the feature maps (corner, edge, and symmetry maps) between the reference and distorted images. Since the image degradation leads to the gradient information change, gradient changes were measured for assessing the image quality [16] with CS. Also in complex wavelet domain, complex wavelet coefficients were compared for IQA using CS [17].

2.2. Human Perception, Saliency, and Visual Attention Based IQMs

A human perception based IQM is motivated by the fact that only the image distortions that can be perceived by most people affects the subjective image quality. This means that if the distortion that cannot be perceived by the HVS occurs with regard to the reference image, people may

consider that the distorted image is the same as or similar to the reference image. Thus, some IQMs use the just-noticeable-distortion to detect the distortion that human eye can perceive. A sharpness metric based on just-noticeable blurs was proposed to measure blur artifacts [18] and a perceptual IQM for blocking artifacts of joint photographic experts group (JPEG) compressed images was proposed [19]. A distortion measure of the effect of frequency distortion, and a noise quality measure (NQM) of the effect of additive noise were developed [20]. DCTune was designed in the context of a discrete cosine transform (DCT)-based model of visual quality [21]. Also, ITU recommended four annexes for objective perceptual IQA [22]. A wavelet based visual signal-to-noise ratio (VSNR) for natural images was also developed based on near-threshold and suprathreshold properties of the human vision [23].

Another approach related to the human perception is based on the phase [24–26]. Phase-based IQMs were motivated from the fact that if an image has some structural distortions, structural distortions lead to the consistent phase change. For IQA, the phase congruency was used [24], which is a measure of feature significance in images and can be used as a method of edge detection that is particularly robust against changes in illumination and contrast. Zhai *et al*. proposed the log Gabor phase similarity [25], which is a FR IQM based on measuring of similarities between phases in the log Gabor transform domain. Also, similarity of phase spectrum was used for IQA [26].

Also visual attention based IQMs were developed [27, 28]. Most existing IQMs do not take the human attention analysis into account. Attention to particular objects or regions is an important fact of human vision and perception system in measuring perceived image and video qualities. Feng *et al*. presented a saliency-based objective quality assessment metric [27], for assessing the perceptual quality of decoded video sequences affected by packet loss. Also, an approach for extracting visual attention regions based on a combination of a bottom-up saliency model and semantic image analysis was proposed [28].

2.3. Information Theoretical IQMs

An information theoretic approach was proposed, which quantifies visual fidelity by means of an information fidelity criterion (IFC) derived based on natural scene statistics [29]. The visual information fidelity (VIF) was also presented [30].

Most conventional IQMs introduced in this section use the entire image pixels. However, if an image is degraded due to the distortions such as image compression, additive noise, and channel error in the transmission systems, distortion of the image is widely distributed over all the image pixels. Therefore, instead of using the whole image pixels, several IQMs use some part of an image [7, 14, 22, 29]. Both the edge peak signal-to-noise ratio (EPSNR) [22] and the VSSIM [7] were presented for the video quality assessment. To evaluate the image quality, these metrics use a small number of pixels instead of the whole image pixels. In the case of VSSIM, local SSIM indices were computed for randomly selected blocks. The EPSNR uses edge pixels because human perceives sensitively intensity variation around edges of an image. Also, the JFSM [14] was presented for assessing the image quality by using selected feature points such as edges, corners, and planar pixels. The estimated PSNR [29], presented for a reduced-reference IQA, uses the representative intensity values in an image to measure the PSNR. This work was motivated by the concept that the whole image pixels are not needed for IQA. The EPSNR and JFSM assume that feature points well reflect the degree of distortion. The VSSIM and estimated PSNR are motivated by the fact that distortion exists globally in the entire image area when an image is degraded. These two cases point out that the whole image pixels are not needed for evaluating the image quality.

In previous work, we presented two IQMs using CS: with derivative filters [16] and the complex wavelets [17]. These IQMs use the CS measurement technique that represents a compressible image by a small number of measurements. Also, in this paper, for assessing the image quality, we use CS combined with a set of filters consisting of gradient filters, LoG filters, and Gabor filters, since outputs of these filters are compressible. In this paper, we propose a new IQM using CS and a set of filters, in which filter selection with regard to the quality measure is proposed.

3. PROPOSED IQM USING CS AND A SET OF FILTERS

In this section, we propose a new IQM using CS and a filter set that consists of gradient filters, LoG filters, and Gabor filters. First, we describe a filter set used in this paper. Second, CS is briefly reviewed and how to use CS for measuring the image quality is explained. Then, a filter selection algorithm is presented.

3.1. Filter Sets

In this paper, we use a set of filters $H = \{h_j,\ 1 \le j \le N_f\}$, where N_f denotes the number of filters, e.g., N_f = 38 consisting of two gradient filters, six LoG filters, and 30 Gabor filters, as used in spectral histogram representation [32]. Each filter has a unique property and thus analysis of several filter outputs can well represent the information on an image.

In general, the filter output $g_{ij}(s,t)$ at pixel (s,t) can be defined as a convolution of an image $f_i(s,t)$, in the image set $F = \{f_1, f_2, \cdots, f_{N_I}\}$ containing N_I images, with a filter $h_j(s,t)$, which can be expres sed as

$$g_{ij}(s,t) = h_j(s,t) * f_i(s,t), \tag{1}$$

where * signifies the convolution operator. The set of filtered images can be written as $G = \{g_{ij},\ 1 \le i \le N_I \text{ and } 1 \le j \le N_f\}$.

Gradients $g_{i1}(s,t)$ and $g_{i2}(s,t)$ at pixel (s,t) along the vertical and horizontal directions are defined a s, respectively

$$\begin{aligned} g_{i1}(s,t) &= h_1(s,t) * f_i(s,t) \\ &= f_i(s-1,t-1) + 2f_i(s,t-1) + f_i(s+1,t-1) \\ &\quad - \big(f_i(s-1,t+1) + 2f_i(s,t+1) + f_i(s+1,t+1)\big), \end{aligned} \tag{2}$$

$$\begin{aligned} g_{i2}(s,t) &= h_2(s,t) * f_i(s,t) \\ &= f_i(s-1,t-1) + 2f_i(s-1,t) + f_i(s-1,t+1) \\ &\quad - \big(f_i(s+1,t-1) + 2f_i(s+1,t) + f_i(s+1,t+1)\big). \end{aligned} \tag{3}$$

The LoG filter is defined as

$$h_j(s,t) = \alpha \times (s^2 + t^2 - \sigma^2) e^{-\frac{s^2+t^2}{\sigma^2}}, \quad 3 \le j \le 8 \tag{4}$$

where σ denotes the standard deviation of the Gaussian filter and six LoG filters with $\sigma = \sqrt{2}, 1, 2\sqrt{2}, 4, 4\sqrt{2}, \text{and } 8$ are used in our experiments.

The Gabor filters [33] have received considerable attention because the characteristics of certain c ells in the visual cortex of some mammals can be approximated by these filters. Gabor filters are constructed by modulating sine/cosine waves with a Gaussian filter. Thus, a Gabor filter can be vi ewed as a sinusoidal plane of particular frequency and orientation. Decomposition of a signal is a ccomplished by using a quadrature pair of Gabor filters, with a real part specified by a cosine wav e modulated by a Gaussian function whereas an imaginary part by a sine wave modulated by a Ga ussian function. The real and imaginary parts are even symmetric and odd symmetric, respectivel y. The Gabor filter is defined as

$$h_j(s,t) = e^{-\frac{1}{2T^2}\left((s\cos\theta+t\sin\theta)^2+(-s\cos\theta+t\sin\theta)^2\right)} \times e^{-\sqrt{-1}\frac{2\pi}{T}(s\cos\theta+t\sin\theta)}, \qquad 9 \le j \le N_f \tag{5}$$

where T and θ signify the scale and orientation, respectively, and 30 Gabor filters with scale T = 2, 4, 8, 14, 22 and orientation θ = 0, 30, 60, 90, 120, 150º are used.

3.2. Review on CS

CS is a technique used for acquiring a signal that is sparse or compressible [34, 35]. CS can be easily performed by a general linear measurement process. Let **x** be an N×1 vector representing image intensity values, **y** be an M×1 vector denoting measurements, and Φ be an M×N measurement matrix. Then, the measurement vector **y** can be defined as

$$\mathbf{y} = \Phi\mathbf{x}, \tag{6}$$

where a measurement matrix Φ is fixed, for example, elements of which have values of '+1' and '–1' with the same probability of '0.5'. Figure 1 shows the CS measurement process [34]. Filter outputs of an image or coefficients of the basis function can be measured using the CS measurement.

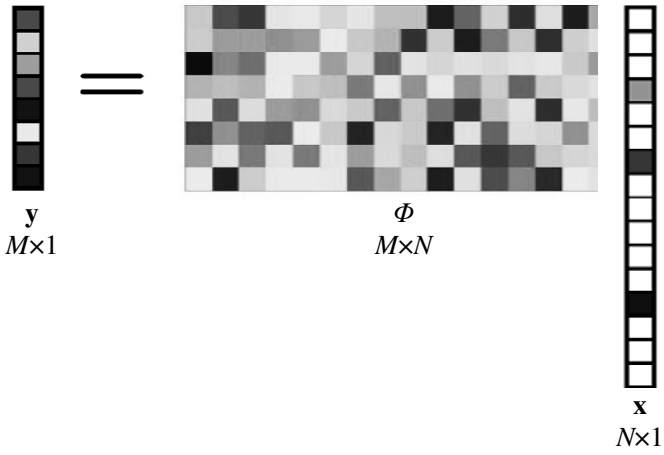

Figure 1. CS measurement process.

In CS, it is important to define how many measurements (M) are required for perfectly reconstruc ting the compressible signal $\mathbf{x}$. If the measurement matrix Φ satisfies the restricted isometry prope rty (RIP) [35], i.e., if only M is generally greater than $2K$, the signal $\mathbf{x}$ can be perfectly reconstruct ed, where K denotes the number of nonzero entries in the signal $\mathbf{x}$. RIP condition of order $2K$ for a ll K-sparse signals $\mathbf{x}_1$ and $\mathbf{x}_2$ is defined as

$$(1-\delta_{2K}) \le \frac{\left\|\Phi\mathbf{x}_1 - \Phi\mathbf{x}_2\right\|_2^2}{\left\|\mathbf{x}_1 - \mathbf{x}_2\right\|_2^2} \le (1+\delta_{2K}), \tag{7}$$

where $\|\cdot\|_2$ represents $L2$ norm of a vector. This means that the distance between the measurements of sparse signals $\mathbf{x}_1$ and $\mathbf{x}_2$ is close to the distance between those sparse signals. Therefore, the comparison of two sparse signals can be replaced by the comparison of measurements of those signals. In this paper, we use the CS measurements for comparing two filter outputs of the reference and distorted images. Then, measurements of each image are compared for measuring the difference between two images.

3.3. Proposed IQM

Figure 2 shows the block diagram of the proposed IQM using CS and a filter set. Figures 2(a) and 2(b) represent the training and measurement processes of the proposed IQM, respectively. In the training process, each of the reference and distorted images is convolved with a filter set, which consists of the gradient, LoG, and Gabor filters, to obtain the sparse filter outputs via CS measurement process. Then, measurements of the reference and distorted images are compared for measuring the quality of the distorted image. If these procedures are performed for all the images in database, the quality measure of each filter can be obtained, and then, filters that are significant for improving the performance are selected by using the proposed filter selection method. In the measurement process, the reference and distorted images are convolved with the selected filter set in the training process in Figure 2(b) to obtain the measurements of the filter outputs. Then, the quality of the distorted image is evaluated by comparing the measurements.

3.3.1. Measurement of Filter Outputs

Let $\mathbf{x}_{ij}$ be a sparse signal lexicographically ordered, consisting of filtered values g_{ij}. Measurement $\mathbf{y}_{ij}$ of $\mathbf{x}_{ij}$ for i-th image and j-th filter can be written as

$$\mathbf{y}_{ij} = \Phi^p \mathbf{x}_{ij}. \tag{8}$$

In Eq. (8), the pixelwise measurement matrix Φ^p is fixed without relation to $\mathbf{x}_{ij}$. Also, measureme nts can be performed blockwise. In this case, measurement $\mathbf{y}_{ij}(v,h)$ at (v,h)-th block for i-th image and j-th filter can be expressed as

$$\mathbf{y}_{ij}(v,h) = \Phi^b \mathbf{x}_{ij}(v,h). \tag{9}$$

The blockwise measurement matrix Φ^b is also fixed without relation to $\mathbf{x}_{ij}(v, h)$.

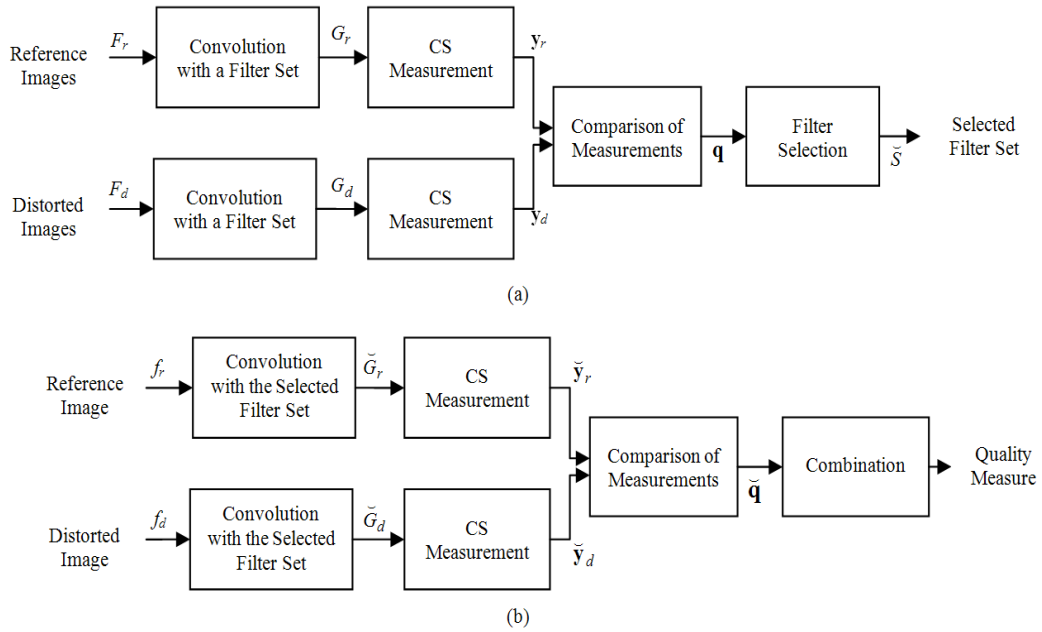

Figure 2. Block diagram of the proposed IQM using CS and a filter set. (a) training process, (b) measurement process.

3.3.2. IQM Based on the PSNR between Measurements

Our proposed IQM is based on the PSNR between measurements of each filter output of the reference and distorted images. The PSNR between pixelwise measurements is defined as

$$PSNR_{ij}^{p} = 10 \times \log\left(\frac{255^2}{\frac{1}{M^{p}} \times \left\| \mathbf{y}_{ij}^{r} - \mathbf{y}_{ij}^{d} \right\|^2} \right), \tag{10}$$

where superscripts r and d signify the reference and distorted images, respectively, and M^{p} denot es the number of pixelwise measurements. In using pixelwise measurements, the overall quality measure q_{ij} for i-th image and j-th filter is equal to $PSNR_{ij}^{p}$ and is written a

$$q_{ij} = PSNR_{ij}^{p}. \tag{11}$$

The PSNR between blockwise measurements at (v, h)-th block is expressed as

$$PSNR_{ij}^{b}(v,h) = 10 \times \log\left(\frac{255^2}{\frac{1}{M^{b}} \times \left\| \mathbf{y}_{ij}^{r}(v,h) - \mathbf{y}_{ij}^{d}(v,h) \right\|^2} \right) \tag{12}$$

where M^{b} denotes the number of blockwise measurements. Then, the overall quality measure ca n be written as

$$q_{ij} = \frac{1}{V_i \times H_i} \sum_{v=1}^{V} \sum_{h=1}^{H} PSNR_{ij}^{b}(v,h), \tag{13}$$

where V_i and H_i represent the numbers of blocks of i-th image along the vertical and horizontal directions, respectively. In this paper, we use the blockwise measurement. Here, the block size is 8×8, which is empirically determined.

3.3.3. Filter Selection

In this paper, we use 38 filters consisting of two gradient filters, six LoG filters, and 30 Gabor filters (with five scales and six orientations). However, all these filters do not effectively reflect the subjective quality as perceived by the human eye. Thus, it is required to select a small number of filters that well reflect the subjective image quality. Also, to use all the filters requires a high computational load, and some filters are not necessary for effective IQA. Therefore, in this paper, we propose a two-step filter selection method that chooses a small number of filters that reflect well the subjective image quality. Before introducing the proposed algorithm, it is required that two image databases used in our experiments be briefly introduced. The image database, called LIVE database [36, 37], includes 29 reference images, 982 degraded images, and their difference mean opinion score (DMOS) values. The distorted images (the image size of typically 768×512) are obtained by JPEG, JPEG2000 (JP2K), white noise in the RGB components (WN), Gaussian blur (GBlur), and transmission errors in the JP2K bit stream using a fast-fading Rayleigh channel model (FF). Also, TID2008 database is used [38]. TID2008 database used in our experiments consists of 25 reference and 1,700 distorted images. The advantage of TID2008 with respect to LIVE database is that TID2008 accounts for 17 different types of distortions, and thus covers more practical applications and known peculiarities of the HVS. Thus, in this paper, the proposed filter selection method considers separately overall performance and performance of each distortion type. Figure 3 shows the pseudo code of our proposed filter selection method, which consists of two steps. Figure 3(a) shows the filter selection process and is performed for each distortion type. Figure 3(b) illustrates the filter elimination process performed for all types of distortions.

First of all, before performing the filter selection step, we normalize the quality measure for each filter using the variance normalization technique [39, 40]. This procedure is accomplished for fitting the scale and distribution of the quality measures for each filter since the quality measures for each filter have different scales and distributions. Thus, the normalized quality measure $\hat{q}_{ij}$ for j-th filter can be defined as

$$\hat{q}_{ij} = \left(\frac{q_{ij} - m_j}{\sigma_j} \right), \tag{14}$$

with

$$m_j = \frac{1}{N_I} \sum_{i=1}^{N_I} q_{ij}, \tag{15}$$

$$\sigma_j = \sqrt{\frac{1}{N_I} \sum_{i=1}^{N_I} (q_{ij} - m_j)^2}, \tag{16}$$

where N_I and N_f denote the number of images and filters, respectively, and m_j and σ_j represent the sample mean and standard deviation of the quality measures q_{ij} for j-th filter with N_I images, respe ctively.

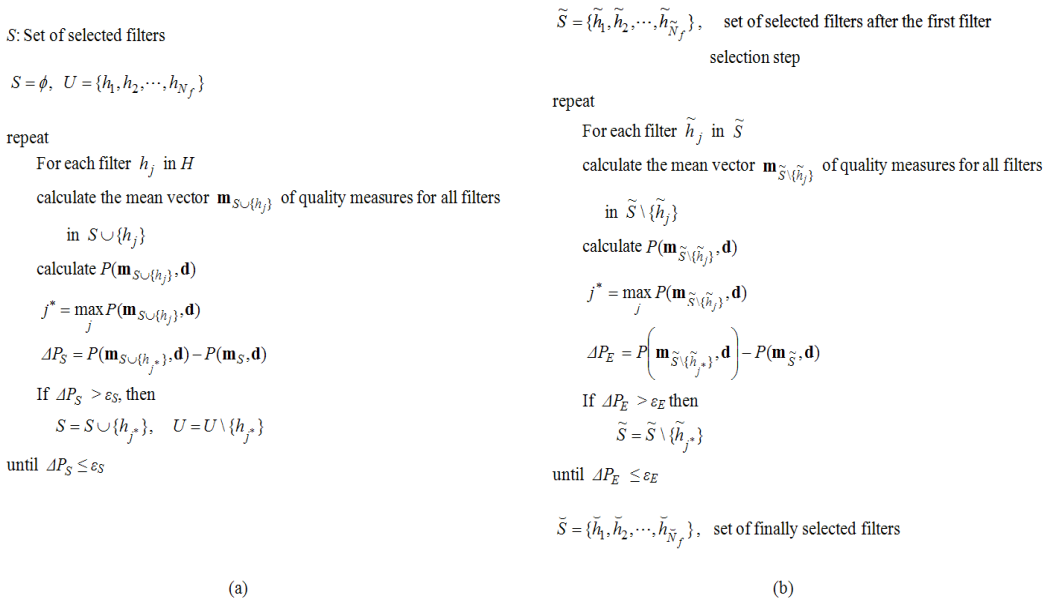

Figure 3. Pseudo code of the proposed filter selection method. (a) filter selection step, (b) filter elimination step.

Next, we will introduce the fidelity of the performance evaluation used for IQA, one of which is t he Pearson correlation coefficient (CC). Let $\hat{\mathbf{q}}_j$ and $\mathbf{d}$ be the vector of normalized quality measur es for j-th filter and vector consisting of DMOS values, respectively, which can be expressed as

$$\hat{\mathbf{q}}_j = \begin{bmatrix} \hat{q}_{1j} & \hat{q}_{2j} & \cdots & \hat{q}_{N_I j} \end{bmatrix}^T, \tag{17}$$

$$\mathbf{d} = \begin{bmatrix} DMOS_1 & DMOS_2 & \cdots & DMOS_{N_I} \end{bmatrix}^T. \tag{18}$$

Then, the Pearson CC between normalized quality measures $\hat{q}_{ij}$ for j-th filter and the DMOS value s can be expressed as

$$P(\hat{\mathbf{q}}_j, \mathbf{d}) = \frac{\sum_{i=1}^{N_I} (\hat{q}_{ij} - \hat{m}_j)(DMOS_i - m_{DMOS})}{\sqrt{\sum_{i=1}^{N_I} (\hat{q}_{ij} - \hat{m}_j)^2} \sqrt{\sum_{i=1}^{N_I} (DMOS_i - m_{DMOS})^2}}, \tag{19}$$

with

$$\hat{m}_j = \frac{1}{N_I} \sum_{i=1}^{N_I} \hat{q}_{ij}, \tag{20}$$

$$m_{DMOS} = \frac{1}{N_I}\sum_{i=1}^{N_I} DMOS_i, \tag{21}$$

where $\hat{m}_j$ and m_{DMOS} denote the mean of normalized quality measures $\hat{q}_{ij}$ for j-th filter and DMOS values, respectively.

Now, we explain the proposed filter selection method. The first step in Figure 3(a) is designed for improving the performance for each distortion type. In the first filter selection step, the filter h_j that gives the maximum Pearson CC between DMOS values and mean values of quality measures for all filters in $S \cup \{h_j\}$ is selected. Here, the mean vector $\mathbf{m}_{S\cup\{h_j\}}$ of quality measures for all filters in $S \cup \{h_j\}$ can be defined as

$$\mathbf{m}_{S\cup\{h_j\}} = \begin{bmatrix} m_1 & m_2 & \cdots & m_{N_I} \end{bmatrix}^T, \tag{22}$$

where m_i denotes the mean of quality measures of all filters in $S \cup \{h_j\}$ for i-th image. It can be expressed as

$$m_i = \frac{1}{N_{S\cup\{h_j\}}}\sum_{j\in S\cup\{h_j\}} q_{ij}, \tag{23}$$

where $N_{S\cup\{h_j\}}$ signifies the number of filters in $S \cup \{h_j\}$. The first step is repeated until the error ΔP_S between $P(\mathbf{m}_{S\cup\{h_{j^*}\}}, \mathbf{d})$ and $P(\mathbf{m}_S, \mathbf{d})$ is greater than a threshold ε_S (ε_S is equal to '0' in our e xperiments), where ΔP_S can be defined as

$$\Delta P_S = P(\mathbf{m}_{S\cup\{h_{j^*}\}}, \mathbf{d}) - P(\mathbf{m}_S, \mathbf{d}). \tag{24}$$

In the proposed filter selection method, other fidelity such as the root mean square error (RMSE) can be used instead of the Pearson CC.

This filter selection step is applied to each distortion type. Thus, if the number of distortion types is N_D (e.g., N_D is equal to 5 and 17 in our experiments of LIVE and TID2008 databases, respectively), filter sets consisting of N_D selected filters are obtained. Thus, a set $\tilde{S}$ of selected filters after the filter selection step can be defined as

$$\tilde{S} = S_1 \cup S_2 \cup \cdots \cup S_{N_D}, \tag{25}$$

with a set $\tilde{S}$ expressed as

$$\tilde{S} = \{\tilde{h}_1, \tilde{h}_2, \cdots, \tilde{h}_{\tilde{N}_f}\}, \tag{26}$$

where $\tilde{N}_f$ denotes the number of the selected filters after the filter selection step (in our experiments, $\tilde{N}_f$ is equal to 10 and 28 for LIVE and TID2008 databases, respectively).

In the filter elimination step shown in Figure 3(b), the filters degrading the overall performance of the proposed IQM are eliminated. Thus, a set $\tilde{S}$ of finally selected filters after the filter

elimination step can be defined as

$$\breve{S} = \{\breve{h}_1, \breve{h}_2, \cdots, \breve{h}_{\breve{N}_f}\}, \tag{27}$$

where $\breve{N}_f$ denotes the number of the selected filters by the proposed filter selection method (in our experiments, $\breve{N}_f$ is equal to 4 and 8 for LIVE and TID2008 databases, respectively). Then, the quality measures for filters in the set $\breve{S}$ are combined for constructing an IQM. This procedure will be presented in Section 3.3.4.

Table 1 lists the performance comparison of the proposed filter selection method for all data and different types of distortions in LIVE database in terms of the Pearson CC. In Table 1, numbers in bold face represent the largest values for each of different distortion types. First of all, Table 1 shows that the Pearson CC values for all data are increased by applying the proposed filter selection method. In terms of the performance for each distortion type, the Pearson CC values for three distortions including JP2K#2, GBlur, and FF distortions are increased by applying the filter selection method.

Table 1. Performance Comparison of the Proposed Filter Selection Method for All Data (LIVE Database) in Terms of the Pearson CC.

	JP2K#1	JP2K#2	JPEG#1	JPEG#2	WN	GBlur	FF	All data
w/o filter selection (N_f=38)	0.9763	0.9652	0.9674	0.9883	0.9822	0.9390	0.8256	0.9248
After 1st step ($\tilde{N}_f$=10)	**0.9857**	0.9805	**0.9760**	**0.9919**	**0.9877**	0.9636	0.9602	0.9522
After 2nd step ($\breve{N}_f$=4)	0.9808	**0.9810**	0.9751	0.9908	0.9851	**0.9699**	**0.9650**	**0.9614**

Table 2 lists the performance comparison of the proposed filter selection method for all data and different types of distortions in TID2008 database in terms of the Spearman rank order CC (SROCC), which was recommended in [41]. For all data in the TID2008, as the proposed filter selection method is applied, the SROCC values are increased. In comparing Table 2 with Table 1, in Table 2, the results obtained after final filter selection are the best for all distortion types while it is not true in Table 1. As previously mentioned, TID2008 consists of the distorted images with 17 distortion types. It is noted that in Table 2, TID2008 database is not practically classified according to the distortion type. Each class among seven classes includes the several distortion types [38]. If TID2008 database is divided into 17 distortions, the results shown in Table 2 might change.

Next, we introduce the saliency to reflect the degree of importance that each pixel or each block has in an image and how to use in the proposed IQM.

Table 2. Performance Comparison of the Proposed Filter Selection Method for All Data (TID2008 Database) in Terms of the SROCC.

	Noise	Noise2	Safe	Hard	Simple	Exotic	Exotic2	All data
w/o filter selection (N_f=38)	0.779	0.783	0.796	0.764	0.804	0.802	0.797	0.786
After 1st step ($\tilde{N}_f$=28)	0.791	0.799	0.811	0.779	0.818	0.807	0.805	0.799
After 2nd step ($\tilde{N}_f$=8)	**0.812**	**0.822**	**0.832**	**0.807**	**0.849**	**0.817**	**0.824**	**0.823**

3.3.4. Saliency-Based Weighting

In an image, each pixel or each block has the different degree of importance in terms of human perception. Thus, each pixel/block must be differently dealt according to the degree of importance that it has. The degree of importance can be represented with the saliency.

In this section, we adapt a saliency-weighting scheme into the proposed IQM. In this paper, we use the graph-based visual saliency method [42] for obtaining the saliency map. If the saliency map is obtained, its values are multiplexed with quality measure values for each block. After this procedure, a new quality measure value q'_{ij} at i-th row and j-th column block is obtained as

$$q'_{ij} = \omega_{ij} \times q_{ij}, \tag{28}$$

where ω_{ij} denotes the saliency value at the corresponding block. The saliency value can be define d as

$$\omega_{ij} = \frac{\frac{1}{V \times H}\sum_{v=1}^{V}\sum_{h=1}^{H} SM_{ij}(v,h)}{\frac{1}{N_R \times N_C}\sum_{k=1}^{N_R}\sum_{l=1}^{N_C} SM(k,l)}, \tag{29}$$

where the SM is the saliency map, V and H are the numbers of rows and columns of each block, and N_R and N_C denote the numbers of rows and columns of the saliency map, respectively. Since each block has the different affectivity for the quality according to the degree of visual attention, this affectivity should be considered in the IQA. Thus, in this paper, we use the saliency-based weights by differently considering each block according to the degree of importance.

Next, we introduce how to combine the quality measures of the selected filters.

3.3.5. Numerical Measure

Next, normalized quality measure values for selected filters are combined into a single quality measure value. Therefore, the proposed metric using compressive sensing and a filter set (CSF) can be defined as

$$CSF = \frac{1}{\breve{N}_f} \sum_{j=1}^{\breve{N}_f} \breve{q}_{ij}, \tag{30}$$

where $\breve{q}_{ij}$ denotes the normalized quality measure for selected filters using the proposed filter selection method.

As general objective IQMs that evaluate the quality of the distorted image, metrics that quantitatively compute differences between the original and distorted images are used. However, these metrics are not necessarily correlated well with the subjective IQA, for example, the DMOS [41]. Consequently, development of the objective IQM that are consistent with the subjective image quality is desirable.

In this paper, a logistic regression [43] is performed to describe the relationship between the DMOS and an IQM. The logistic regression can be written as

$$\text{DMOS} = a_1 \left(\frac{1}{2} - \frac{1}{1 + e^{(a_2 \times (IQM - a_3))}} \right) + a_4 \times IQM + a_5, \tag{31}$$

where parameters a_1, a_2, a_3, a_4, and a_5 denote constants obtained after logistic regression. For testing the performance of an IQM obtained after fitting by logistic regression method, the fitted versions of the IQM are compared with the DMOS, the subjective IQA method, in terms of the performance measure such as the Pearson CC, RMSE, SROCC and Kendall CC, which were recommended by video quality expert group (VQEG) [43] and used in [38]. For each conventional IQM, Eq. (31) is used. After fitting them, the fitted versions are compared with the DMOS.

4. EXPERIMENTAL RESULTS AND DISCUSSIONS

In this paper, we propose a new IQM using CS and a filter set. To evaluate the performance of the proposed metric, we use the LIVE [36] and TID2008 [38] databases.

4.1. Experiments on LIVE Database

In experiments on LIVE database, we use only 779 images excluding 203 original images among 982 images. The measurement process is performed block by block with 8×8 block size and M is empirically set to 16. To evaluate the performance of the proposed metric, the Pearson CC, RMSE, and SROCC, recommended in VQEG [43], between IQM values and DMOS values are used. The Pearson CC between the IQM and the DMOS is calculated to evaluate the prediction accuracy. The higher the Pearson CC between an IQM and the MOS (or DMOS) is, the better the metric is. The RMSE quantifies the amount of the distance between the true values and the estimates. If it is small, then image quality is close to the MOS (or DMOS). The SROCC can reflect the monotonicity of the IQM. Thus, if the SROCC between the IQM and the DMOS is high, the metric is good. Also, the performance of our proposed metric is evaluated via comparison of the proposed metric with nine conventional IQMs such as the PSNR, MSVD [11], HRQM [13], MSSSIM [6], NQM [20], DCTune [21], IFC [29], VIF [30], and DFCS [16]. In this paper, we propose two IQMs: CSFs without weights and with weights based on the saliency information.

Table 3 shows the performance comparison of 11 IQMs in terms of the Pearson CC after logistic regression. For the entire images, the proposed CSF with weights gives better results than the other conventional IQMs, which means that the proposed CSF with weights is the most similar to the DMOS (highest Pearson CC) among 11 IQMs. For the JP2K, JPEG, and WN distorted images, the proposed CSF with weights gives better performance than the other IQMs. For other distortion types, VIF (for GBlur and FF distortions) gives better performance than the other IQMs. However, for the GBlur distortion, the proposed CSF without weights shows better performance than the other IQMs except for the VIF. For the FF distortion, both the proposed CSF methods with and without weights give the performances comparable to the VIF. Two proposed CSF methods with and without weights give better performances than other conventional IQMs. The saliency-based weighted CSF is better than the CSF without weights.

Table 3. Performance Comparison of 11 IQMs in Terms of the Pearson CC after Logistic Regression (LIVE Database).

	JP2K#1	JP2K#2	JPEG#1	JPEG#2	WN	GBlur	FF	All data
PSNR	0.9332	0.8740	0.8856	0.9167	0.9859	0.7834	0.8895	0.8709
MSVD [11]	0.9733	0.9582	0.9350	0.9783	0.9738	0.7937	0.9264	0.8773
HRQM [13]	0.9029	0.9188	0.8776	0.9500	0.9458	0.9394	0.9354	0.9051
MSSSIM [6]	0.9702	0.9711	0.9699	0.9879	0.9737	0.9487	0.9304	0.9393
NQM [20]	0.9508	0.9463	0.9387	0.9783	0.9885	0.8858	0.8367	0.9075
DCTune [21]	0.8486	0.7834	0.8825	0.9418	0.9288	0.7095	0.7693	0.8046
IFC [29]	0.9421	0.9626	0.9209	0.9744	0.9766	0.9691	0.9631	0.9441
VIF [30]	0.9791	0.9787	0.9714	0.9885	0.9877	**0.9762**	**0.9704**	0.9533
DFCS [16]	0.9818	0.9811	0.9764	0.9904	0.9857	0.9687	0.9637	0.9575
CSF w/o weights	0.9808	0.9810	0.9751	0.9908	0.9851	0.9699	0.9650	0.9614
CSF w/ weights	**0.9840**	**0.9815**	**0.9766**	**0.9920**	**0.9902**	0.9671	0.9684	**0.9635**

Table 4 lists the performance comparison of 11 different IQMs in terms of the RMSE. Table 4 shows the similar results to Table 3. The proposed CSF with weights gives better performance than the conventional IQMs for JP2K and JPEG distorted images, which signifies that the distance between the CSF and DMOS is small at least for JP2K, JPEG, and WN distortion types. For the GBlur and FF distortions, the VIF gives the best results. CSF with saliency-based weights is totally better than the CSF without weights and other IQMs.

Table 4. Performance Comparison of 11 IQMs in Terms of the RMSE after Logistic Regression (LIVE Database).

	JP2K#1	JP2K#2	JPEG#1	JPEG#2	WN	GBlur	FF	All data
PSNR	8.4858	12.7437	10.7793	13.5633	4.6689	11.4402	12.9716	13.4265
MSVD [11]	5.4453	7.5459	8.2818	7.0752	6.3575	11.2364	10.7233	13.1106
HRQM [13]	10.2034	10.4176	11.1933	10.6590	9.0870	6.3313	10.0721	11.6163
MSSSIM [6]	5.7214	6.2584	5.6575	5.2729	6.3577	5.8225	10.4023	9.3691
NQM [20]	7.3167	8.4762	8.0004	7.0336	4.2250	8.5413	15.5467	11.4698
DCTune [21]	12.4881	16.2971	10.9168	11.4089	10.3340	12.9712	18.1366	16.2150
IFC [29]	7.9184	7.1050	9.0470	7.6267	5.9990	4.5380	7.6398	9.0007
VIF [30]	4.7986	5.3864	5.5083	5.1274	4.3598	**3.9905**	**6.8553**	8.2459
DFCS [16]	4.5136	5.1067	4.8576	4.7140	4.7071	4.5840	7.6121	8.0513
CSF w/o weights	4.6338	5.1170	3.9406	4.6233	4.8160	4.4980	7.4671	7.5153
CSF w/ weights	**4.2375**	**5.0577**	**4.0241**	**4.3066**	**3.8973**	4.6966	7.1677	**7.3156**

Table 5 lists the performance comparison of different IQMs in terms of the SROCC. Similarly to Tables 3 and 4, Table 5 shows that the proposed CSF with weights gives better performance than other IQMs for all data. For JP2K#1, JPEG#2, and FF distortions, the CSF without weights is the best metric among 11 IQMs. The CSF with weights outperforms the other IQM for JPEG#1. For WN and GBlur distortions, the proposed CSFs give the comparable performance to the VIF. Especially, the PSNR and NQM show the best performance for the WN distortion type and the proposed CSFs are comparable to the PSNR and NQM. The proposed CSFs give the best performance among 11 IQMs for the entire images.

Table 5. Performance Comparison of 11 IQMs in Terms of the SROCC after Logistic Regression (LIVE Database).

	JP2K#1	JP2K#2	JPEG#1	JPEG#2	WN	GBlur	FF	All data
PSNR	0.9263	0.8549	0.8779	0.7708	**0.9854**	0.7823	0.8907	0.8755
MSVD [11]	0.9701	0.9414	0.9244	0.8023	0.9786	0.7792	0.9269	0.8772
HRQM [13]	0.9052	0.9127	0.8588	0.8919	0.9287	0.9473	0.9374	0.9056
MSSSIM [6]	0.9645	0.9648	0.9702	0.9454	0.9805	0.9519	0.9395	0.9527
NQM [20]	0.9465	0.9393	0.9360	0.8988	**0.9854**	0.8467	0.8171	0.9049
DCTune [21]	0.8335	0.7209	0.8702	0.8200	0.9324	0.6721	0.7675	0.8032
IFC [29]	0.9386	0.9534	0.9107	0.9005	0.9625	0.9637	0.9556	0.9459
VIF [30]	0.9721	0.9719	0.9699	0.9439	0.9828	**0.9706**	0.9649	0.9584
DFCS [16]	0.9747	**0.9759**	0.9717	0.9488	0.9852	0.9680	0.9620	0.9635
CSF w/o weights	**0.9776**	0.9735	0.9733	**0.9507**	0.9779	0.9698	**0.9664**	0.9639
CSF w/ weights	0.9770	0.9737	**0.9742**	0.9460	0.9853	0.9678	0.9652	**0.9669**

4.2. Experiments on TID2008 Database

In our experiments on TID2008 database, we use the SROCC and Kendall CC for evaluating the performance of 11 IQMs. The Kendall CC is used to measure the degree of correspondence between two rankings. The higher the Kendall CC [38] an IQM has, the better the IQM is.

Table 6 lists the performance comparison of 11 IQMs for the TID2008 database in terms of the SROCC. For all data, MSSSIM gives the best performance. The proposed CSF without weights gives the good performance next to the MSSSIM for all data.

Table 6. Performance Comparison of IQMs in Terms of the SROCC (TID2008 Database).

	Noise	Noise2	Safe	Hard	Simple	Exotic	Exotic2	All data
PSNR	0.704	0.612	0.689	0.697	0.799	0.248	0.308	0.525
MSVD [11]	0.735	0.676	0.757	0.659	0.863	0.281	0.403	0.624
HRQM [13]	0.725	0.761	0.793	0.801	0.843	0.056	0.362	0.607
MSSSIM [6]	0.813	0.850	0.849	**0.874**	0.898	0.728	0.711	**0.853**
NQM [20]	0.865	0.887	0.896	0.733	0.903	0.602	0.432	0.624
DCTune [21]	0.864	0.881	0.877	0.703	0.902	0.529	0.260	0.476
IFC [29]	0.663	0.743	0.775	0.736	0.817	0.269	0.276	0.569
VIF [30]	0.820	0.900	0.908	0.844	0.935	0.531	0.671	0.750
DFCS [16]	0.770	0.777	0.786	0.766	0.798	0.772	0.776	0.778
CSF w/o weights	0.812	0.822	0.832	0.807	0.849	**0.817**	**0.824**	0.823
CSF w/ weights	**0.906**	**0.931**	**0.945**	0.770	**0.952**	0.589	0.706	0.816

Table 7 lists the performance comparison of 11 IQMs for the TID2008 database in terms of the Kendall CC. Similar to results shown in Table 6, for all data, the MSSSIM gives the best performance. The proposed CSF without weights gives the good performance next to the MSSSIM for all data.

In summary, it can be observed that the performance of the proposed CSFs is better than those of conventional IQMs for the LIVE and TID2008 databases. Especially, as shown in Tables 3–5, the proposed CSFs give the superior performance for JP2K and JPEG distortions to nine conventional IQMs for the LIVE database. Also, as shown in Tables 6 and 7, the proposed CSFs are good IQMs among 11 IQMs for the TID2008 database. As shown in experiments on two databases, the proposed CSFs give improved performance regardless of database.

Table 7. Performance Comparison of IQMs in Terms of the Kendall CC (TID2008 Database).

	Noise	Noise2	Safe	Hard	Simple	Exotic	Exotic2	All data
PSNR	0.501	0.424	0.486	0.516	0.598	0.178	0.225	0.369
MSVD [11]	0.538	0.488	0.559	0.476	0.677	0.222	0.320	0.465
HRQM [13]	0.531	0.562	0.595	0.602	0.645	0.050	0.249	0.442
MSSSIM [6]	0.609	0.650	0.649	**0.676**	0.719	0.522	0.604	**0.654**
NQM [20]	0.673	0.704	0.713	0.541	0.720	0.428	0.288	0.461
DCTune [21]	0.683	0.711	0.701	0.527	0.735	0.357	0.170	0.372
IFC [29]	0.477	0.547	0.581	0.552	0.624	0.156	0.208	0.426
VIF [30]	0.634	0.729	0.742	0.660	0.776	0.370	0.499	0.586
DFCS [16]	0.579	0.584	0.593	0.574	0.602	0.580	0.584	0.585
CSF w/o weights	0.645	0.652	0.663	0.641	0.679	**0.647**	**0.652**	0.653
CSF w/ weights	**0.732**	**0.774**	**0.790**	0.593	**0.802**	0.415	0.520	0.647

5. CONCLUSIONS

In this paper, we propose a new IQM CSF, which uses CS and a filter set consisting of the gradient, LoG, and Gabor filters. The proposed CSF converts an image into a compressible signal using a filter set and uses CS for measuring the information of the converted compressible image signal. To reduce the computational time due to the usage of 38 filters and to improve the performance of the proposed CSF, we propose a two-step filter selection method. Also, to reflect visual property in the proposed CSF, we use the saliency-based weights. Through experiments with the LIVE and TID2008 databases, it can be observed that the proposed CSFs with and without the weights give better performance than other conventional IQMs in terms of the Pearson CC, RMSE, and SROCC for LIVE database whereas in terms of the SROCC and Kendall CC for TID2008 database. Future work will focus on the extension of the proposed CSF using color information.

ACKNOWLEDGEMENTS

This work was supported in part by the BK 21 Project.

REFERENCES

[1] Z. Wang and A. C. Bovik, "Mean squared error: Love it or leave it?– A new look at signal fidelity measures," *IEEE Signal Processing Magazine*, vol. 26, no. 1, pp. 98–117, Jan. 2009.

[2] Z. Wang and A. C. Bovik, "A universal image quality index," *IEEE Signal Processing Letters*, vol. 9, no. 3, pp. 81–84, Mar. 2002.

[3] Z. Wang and A. C. Bovik, "Image quality assessment: From error visibility to structural similarity," *IEEE Trans. Image Processing*, vol. 13, no. 4, pp. 600–612, Apr. 2004.

[4] G.-H. Chen, C.-L. Yang, and S.-L. Xie, "Edge-based structural similarity for image quality assessment," in *Proc. Int. Conf. Acoustics, Speech, and Signal Processing 2006*, vol. 2, pp. 14–19, Toulouse, France, May 2006.

[5] G.-H. Chen, C.-L. Yang, and S.-L. Xie, "Gradient-based structural similarity for image quality assessment," in *Proc. Int. Conf. Image Processing*, pp. 2929–2932, Atlanta, GA, USA, Oct. 2006.

[6] Z. Wang, E. P. Simoncelli, and A. C. Bovik, "Multiscale structural similarity for image quality assessment," in *Proc. IEEE Asilomar Conf. Signals, Systems, and Computers*, vol. 2, pp. 1398–1402, Pacific Grove, CA, USA, Nov. 2003.

[7] Z. Wang, L. Lu, and A. C. Bovik, "Video quality assessment based on structural information measurement," *Signal Processing: Image Communication*, vol. 19, no. 2, pp. 121−132, Feb. 2004.

[8] F. Wei, X. Gu, and Y. Wang, "Image quality assessment using edge and contrast similarity," in *Proc. IEEE Int. Joint Conf. Neural Networks*, pp. 852–855, Hong Kong, China, June 2008.

[9] G. Zhai, W. Zhang, X. Yang, and Y. Xu, "Image quality assessment metrics based on multi-scale edge presentation," in *Proc. IEEE Workshop Signal Processing System Design and Implementation*, pp. 331−336, Athens, Greece, Nov. 2005.

[10] C.-L. Yang, W.-R. Gao, and L.-M. Po, "Discrete wavelet transform-based structural similarity for image quality assessment," in *Proc. IEEE Int. Conf. Image Processing*, pp. 377−380, San Diego, CA, USA, Oct. 2008.

[11] A. Shnayderman, A. Gusev, and A. M. Eskicioglu, "An SVD-based grayscale image quality measure for local and global assessment," *IEEE Trans. Image Processing*, vol. 15, no. 2, pp. 422–429, Feb. 2006.

[12] H.-S. Han, D.-O Kim, and R.-H. Park, "Structural information-based image quality assessment using LU factorization," *IEEE Trans. Consumer Electronics*, vol. 55, no. 1, pp. 165–171, Feb. 2009.

[13] D.-O Kim and R.-H. Park, "New image quality metric using the Harris response," *IEEE Signal Processing Letters*, vol. 16, no. 7, pp. 616–619, July 2009.

[14] D.-O Kim and R.-H. Park, "Joint feature-based visual quality assessment," *Electron. Letters*, vol. 43, no. 21, pp. 1134−1135, Oct. 2007.

[15] L. Cui and A. R. Allen, "An image quality metric based on corner, edge and symmetry maps," in *Proc. British Machine Vision Conf.*, Leeds, UK, Sep. 2008.

[16] D.-O Kim, R.-H. Park, and J. W. Lee, "New image quality metric using derivative filters and compressive sensing," in *Proc. 2010 IEEE Int. Conf. Image Processing*, pp. 3357−3360, Hong Kong, China, Sep. 2010.

[17] D.-O Kim and R.-H. Park, "Evaluation of image quality using dual-tree complex wavelet transform and compressive sensing," *Electron. Lett*., vol. 46, no. 7, pp. 494–495, Apr. 2010.

[18] R. Ferzli and L. J. Karam, "A no-reference objective image sharpness metric based on just-noticeable blur and probability summation," in *Proc. Int. Conf. Image Processing*, pp. 445–448, San Antonio, TX, USA, Sept. 2007.

[19] S. Ji, L. Qin, and G. Erlebacher, "Hybrid no-reference natural image quality assessment of noisy, blurry, JPEG2000, and JPEG images," *IEEE Trans. Image Processing*, vol. 20, no. 8, pp. 2089–2098, Aug. 2011.

[20] N. Damera-Venkata, T. Kite, W. Geisler, B. Evans, and A. C. Bovik, "Image quality assessment based on a degradation model," *IEEE Trans. Image Processing*, vol. 9, no. 4, pp. 636–650, Apr. 2000.

[21] A. B. Watson, "DCTune: A technique for visual optimization of DCT quantization matrices for individual images," *Society for Information Display Digest of Technical Papers*, vol. XXIV, pp. 946–949, 1993.

[22] ITU-R Recommendation J.144, "Objective perceptual video quality measurement techniques for digital cable television in the presence of a full reference," *International Telecommunication Union*, Mar. 2004.

[23] D. M. Chandler and S. S. Hemami, "VSNR: A wavelet-based visual signal-to-noise ratio for natural

images," *IEEE Trans. Image Processing*, vol. 16, no. 9, pp. 2284−2298, Sept. 2007.

[24] Z. Liu and R. Laganiere, "On the use of phase congruency to evaluate image similarity," in *Proc. Int. Conf. Acoustics, Speech, Signal Processing*, pp. 937−940, Toulouse, France, May 2006.

[25] G. Zhai, W. Zhang, Y. Xu, and W. Lin, "LGPS: Phase based image quality assessment metric," in *Proc. IEEE Workshop Signal Processing Systems*, pp. 605−609, Shanghai, China, Oct. 2007.

[26] P. Skurowski and A. Gruca, "Image quality assessment using phase spectrum correlation," *Lecture Notes in Computer Science, Computer Vision and Graphics,* Eds. G. Goos *et al.*, Springer-Verlag Berlin Heidelberg, vol. 5337, pp. 80−89, Nov. 2008.

[27] X. Feng, T. Liu, D. Yang, and Y. Wang, "Saliency inspired full-reference quality metrics for packet-loss-impaired video," *IEEE Trans. Broadcasting*, vol. 57, no. 1, pp. 81–88, Mar. 2011.

[28] Z. You, A. Perkis, M. M. Hannuksela, and M. Gabbouj, "Perceptual quality assessment based on visual attention analysis," in *Proc. ACM Int. Conf. Multimedia*, pp. 561−564, Beijing, China, Oct. 2009.

[29] H. R. Sheikh, A. C. Bovik, and G. de Veciana, "An information fidelity criterion for image quality assessment using natural scene statistics," *IEEE Trans. Image Processing*, vol. 14, no. 12, pp. 2117–2128, Dec. 2005.

[30] H. R. Sheikh and A. C. Bovik, "Image information and visual quality," *IEEE Trans. Image Processing*, vol. 15, no. 2, pp. 430–444, Feb. 2006.

[31] T. Goodall and A. C. Bovik, "No-reference task performance prediction on distorted LWIR images," in *Proc. 2014 IEEE Southwest Symposium Image Analysis and Interpretation*, San Diego, CA, USA, Apr. 2014.

[32] X. Liu and D. Wang, "A spectral histogram model for textons and texture discrimination," in *Proc. Int. Joint Conf. Neural Networks*, vol. 2, pp. 1083−1088, Washington, DC, USA, July 2001.

[33] B. Jähne, *Digital Image Processing*. Berlin, Germany: Springer, 6th Ed., 2005.

[34] R. G. Baraniuk, "Compressive sensing," *IEEE Signal Processing Magazine*, vol. 24, no. 4, pp. 118−124, July 2007.

[35] M. F. Duarte, M. A. Davenport, D. Takhar, J. N. Laska, T. Sun, K. F. Kelly, and R. G. Baraniuk, "Single pixel imaging via compressive sampling," *IEEE Signal Processing Magazine*, vol. 25, no. 2, pp. 83–91, Mar. 2008.

[36] H. R. Sheikh, Z. Wang, L. Cormack, and A. C. Bovik, "LIVE image quality assessment database release 2," http://live.ece.utexas.edu/ research/quality.

[37] H. R. Sheikh, M. F. Sabir, and A. C. Bovik, "A statistical evaluation of recent full reference image quality assessment algorithms," *IEEE Trans. Image Processing*, vol. 15, no. 11, pp. 3441–3452, Nov. 2006.

[38] N. Ponomarenko, M. Carli, V. Lukin, K. Egiazarian, J. Astola, and F. Battisti, "Color image database for evaluation of image quality metrics," in *Proc. Int. Workshop Multimedia Signal Processing*, pp. 403−408, Cairns, Queensland, Australia, Oct. 2008.

[39] C.-P. Chen, K. Filali, and J. A. Bilmes, "Frontend postprocessing and backend model enhancement on the Aurora," in *Proc. Int. Conf. Spoken Language Processing*, pp. 241–244, Denver, CL, USA, Sept. 2002.

[40] L. Mingna and Y. Xin, "Image quality assessment by decision fusion," *IEICE Electron. Express*, vol. 5, no. 15, pp. 537−542, Aug. 2008.

[41] ITU-T Recommendation BT.500-11, "Methodology for the subjective assessment of the quality of television pictures," *International Telecommunication Union*, Jan. 2002.

[42] J. Harel, C. Koch, and P. Perona, "Graph-based visual saliency," *Advanced in Neural Information Processing Systems 19*, MIT Press, pp. 545–552, 2007.

[43] VQEG, "Draft final report from the video quality experts group on the validation of objective models of multimedia quality assessment, phase I," http://www.vqeg.org/, 2008.